УНИВЕРЗИТЕТ У БЕОГРАДУ – ГРАЂЕВИНСКИ ФАКУЛТЕТ
UNIVERSITY OF BELGRADE – FACULTY OF CIVIL ENGINEERING

УНИВЕРЗИТЕТ ЦРНЕ ГОРЕ – ГРАЂЕВИНСКИ ФАКУЛТЕТ
UNIVERSITY OF MONTENEGRO – FACULTY OF CIVIL ENGINEERING

САВРЕМЕНИ ПРОБЛЕМИ ТЕОРИЈЕ КОНСТРУКЦИЈА
CONTEMPORARY PROBLEMS OF THEORY OF STRUCTURES

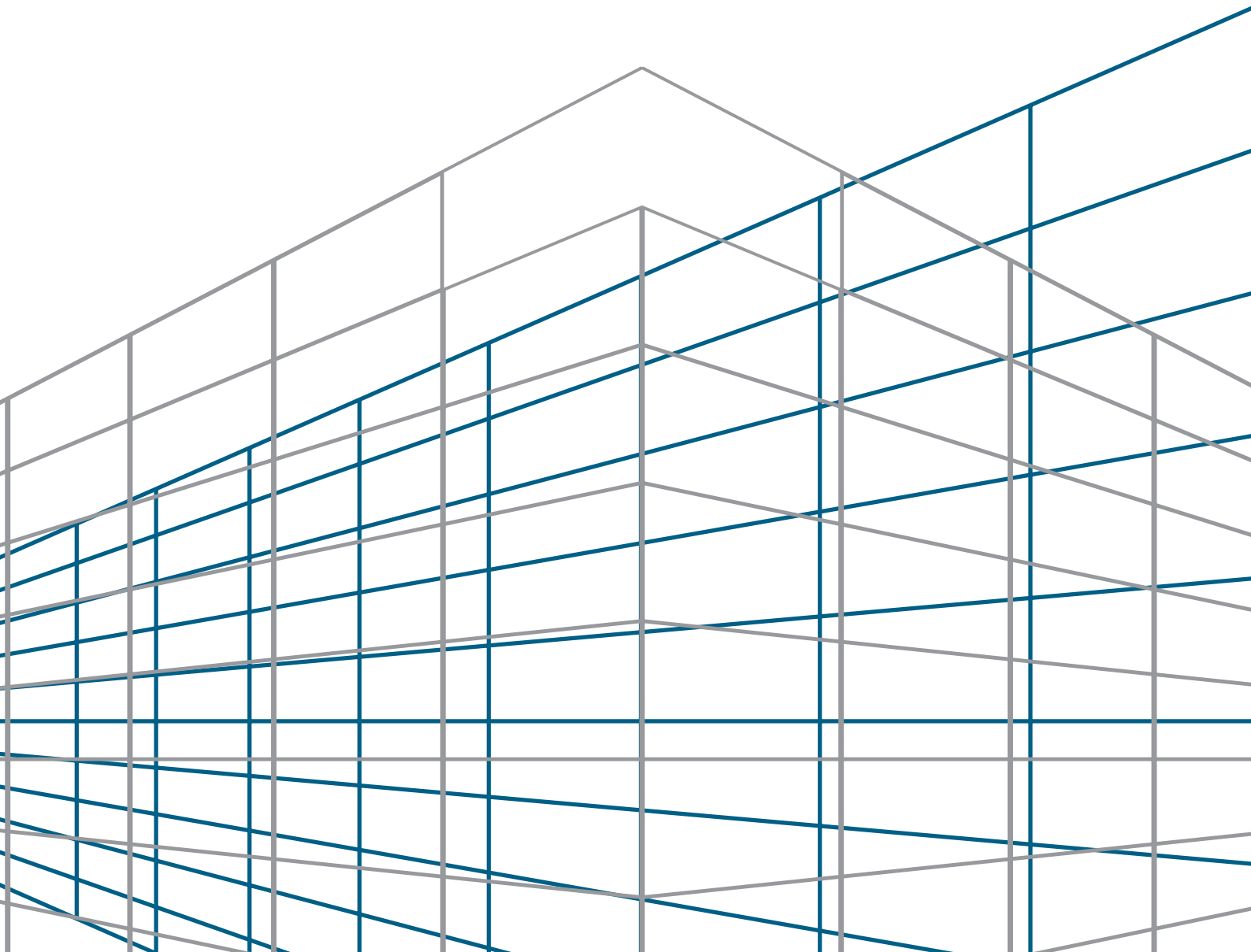

УНИВЕРЗИТЕТ У БЕОГРАДУ - ГРАЂЕВИНСКИ ФАКУЛТЕТ
UNIVERSITY OF BELGRADE - FACULTY OF CIVIL ENGINEERING

УНИВЕРЗИТЕТ ЦРНЕ ГОРЕ - ГРАЂЕВИНСКИ ФАКУЛТЕТ
UNIVERSITY OF MONTENEGRO - FACULTY OF CIVIL ENGINEERING

САВРЕМЕНИ ПРОБЛЕМИ ТЕОРИЈЕ КОНСТРУКЦИЈА

Монографија посвећена успомени на професора Ђорђа Вуксановића

CONTEMPORARY PROBLEMS OF THEORY OF STRUCTURES

Monograph dedicated to the memory of Professor Djordje Vuksanović

Уредници / Editors

Проф. др Мира Петронијевић

Проф. др Бошко Стевановић

Проф. др Марина Ракочевић

Београд, 2016.

Издавачи / Publishers
УНИВЕРЗИТЕТ У БЕОГРАДУ - ГРАЂЕВИНСКИ ФАКУЛТЕТ
UNIVERSITY OF BELGRADE - FACULTY OF CIVIL ENGINEERING

УНИВЕРЗИТЕТ ЦРНЕ ГОРЕ - ГРАЂЕВИНСКИ ФАКУЛТЕТ
UNIVERSITY OF MONTENEGRO - FACULTY OF CIVIL ENGINEERING

За издавача / For the publisher
Проф. др Бранко Божић
Проф. др Милош Кнежевић

Суиздавач / Co-publisher
АГМ КЊИГА, БЕОГРАД

За суиздавача / For the co-publisher
Славица Сарић-Ахмић

Уредници / Editors
Проф. др Мира Петронијевић
Проф. др Бошко Стевановић
Проф. др Марина Ракочевић

Рецензенти / Reviewers
Проф. др Милош Којић
Проф. др Драган Милашиновић
Проф. др Младен Улићевић

Техничка припрема / Technical preparation
Асист. Мирослав Марјановић

Дизајн корица / Cover design
мр Сузана Пајовић

Штампа / Printing
Анаграм студио, Земун

Тираж 500 примерака
Number of copies 500

ISBN 978-86-86363-69-5

Günther MESCHKE, Djordje VUKSANOVIĆ, Miroslav MARJANOVIĆ

FINITE ELEMENT ANALYSIS OF PROPAGATING DELAMINATION IN LAMINATED COMPOSITE PLATES

АНАЛИЗА ШИРЕЊА ДЕЛАМИНАЦИЈЕ У ЛАМИНАТНИМ КОМПОЗИТНИМ ПЛОЧАМА ПРИМЕНОМ МЕТОДЕ КОНАЧНИХ ЕЛЕМЕНАТА

Prof. Dr. techn. Günther MESCHKE
Full Professor at the Institute for Structural Mechanics, Ruhr University Bochum, Germany

Born in 1958, received PhD degree from Vienna University of Technology in 1989. Prof. Meschke is a member of the German Academy of Science and Engineering and of the Academy of Sciences and the Arts of North Rhine-Westphalia. He is Head of the Institute for Structural Mechanics at Ruhr University Bochum and Speaker of the Collaborative Research Center SFB 837 "Interaction Modeling in Mechanized Tunneling". His research in the area of computational structural mechanics is focused on multi-scale and multi-field models of materials and structures as well as advanced discretization methods in civil and geotechnical engineering.

Djordje VUKSANOVIĆ, PhD Civil Eng.
Full Professor at the Faculty of Civil Engineering, University of Belgrade

Born in 1951, received PhD degree from Faculty of Civil Engineering, University of Belgrade in 1988. He was a member of the Serbian Academy of Engineering Sciences, full professor in the field of Theory of Structures and the Dean of the Faculty of Civil Engineering in Belgrade for 8 years. Research fields: FEM, nonlinear analysis of concrete plates, theory of composite plates and shells.

Miroslav MARJANOVIĆ, MSc Civil Eng.
Teaching Assistant at the Faculty of Civil Engineering, University of Belgrade

Born in 1986, BSc in 2009 and MSc in 2010 at Faculty of Civil Engineering, University of Belgrade. Presently, Teaching Assistant in the field of Theory of Structures. Research fields: theory of composite plates and shells, FEM, nonlinear analysis of structures.

Summary

In the paper, an algorithm to track a moving delamination front of arbitrary shape is proposed, which allows considering of arbitrary meshes composed of 4- and 9-node quadrilateral finite elements. The proposed model is developed in the context of a layered finite element plate model. To prevent interlaminar penetration of adjacent layers in the delaminated region, a contact algorithm proposed by the authors is adopted. The model performance is demonstrated by re-analyses of the Double-Cantilever-Beam problem, for which analytical solutions exist, and by transient analyses of laminated composite plates with propagating delamination fronts.

Keywords: propagation, composite plate, layered finite element, transient analysis

Резиме

У овом раду приказан је алгоритам за праћење промене фронта деламинације, који омогућава примену произвољних мрежа четвороугаоних коначних елемената са 4 или 9 чворова. Предложени модел заснован је на слојевитим коначним елементима плоче. Како би се спречило преклапање слојева у зони деламинације, усвојен је контактни алгоритам који су предложили аутори. Примена модела показана је на примеру двоструке конзоле (за коју већ постоји аналитичко решење), као и у динамичкој анализи ламинатних композитних плоча са фронтом деламинације који се шири.

Кључне речи: пропагација, композитна плоча, слојевити коначни елемент, динамичка анализа

1. INTRODUCTION

Laminated composites play an important role in the construction of efficient and lightweight structures and components in mechanical, aeronautical and civil engineering. Examples are high performance parts of aircrafts, wind turbines, ships, cars etc. However, structural defects of such structures (usually in the form of delamination) lead to a considerable reduction of the loading capacity of the composite member. An overview on this common problem of composite structures is given in [1].

The finite element model based on the Generalized Layerwise Plate Theory (GLPT) [2] is capable to conveniently describe the independent motion of the adjacent layers in the delaminated zone. Using the GLP Theory, the relative displacements between the upper and lower portions of the composite laminate in the delaminated zone can be achieved, allowing placing an interface element between adjacent "layers" in the plate formulation. This formulation also allows the calculation of three components G_I, G_{II} and G_{III} of the Strain Energy Release Rate (the energy dissipated during the propagation of delamination per unit of a newly created delaminated area). In order to predict delamination growth, the calculated G_i components are compared with the interlaminar fracture toughness, which is experimentally obtained material property.

In previous investigations, the authors developed a numerical model based on the GLPT for the numerical analysis of free vibrations [3, 4] and the transient response [5] of delaminated composite and sandwich plates and shells. Although a number of computational strategies exist for the modeling of delamination growth (see [6] and references therein), the propagating delamination was not considered in [3, 5].

In this paper, the step-by-step propagation of the previously imposed delaminated zone is accounted using the Virtual Crack Closing Technique (VCCT) [7, 8], which is an approximate method derived from the more fundamental Crack Closure Technique (CCT), assuming that the strain energy released during the delamination growth is equal to the work required to close the crack to its original length (see [9] and references herein). The presented method extends the algorithm previously proposed by Xie et al. [10, 11] and applied by Hosseini-Toudeshky et al. in Refs. [20-22], which was restricted to structured finite element meshes of quadrilateral elements. In this work the VCCT approach is extended to the unstructured meshes of linear and quadratic quadrilateral finite elements. Our algorithm [12] has been implemented in a recently developed MATLAB code for the static and dynamic analysis of damaged composite plates [13]. For the generation of the numerical models and the post-processing of the results, the Pre- and Post-processing program GiD [14] is used.

2. LAYERED FINITE ELEMENT MODEL

In the paper, we consider laminated composite plates made of n orthotropic laminae. Although not necessary, it is convenient to adopt the mid-plane Ω of the laminate as reference x-y plane of the problem. The z-axis is oriented orthogonal to the x-y plane according to a right handed orthonormal coordinate system. The plate thickness is denoted as h (see Figure 1), while the thickness of the k^{th} lamina is denoted as h_k. The plate is supported along the portion Γ_u of the boundary Γ and loaded with loading q acting perpendicular to the mid-plane of the laminate. Note that the previously imposed delaminated zone Ω_{DEL} may change its shape during the loading process, while debonding of the boundary nodes is only possible along free plate boundaries. However, the growth of the delamination cannot change the essential boundary conditions along Dirichlet boundaries Γ_u.

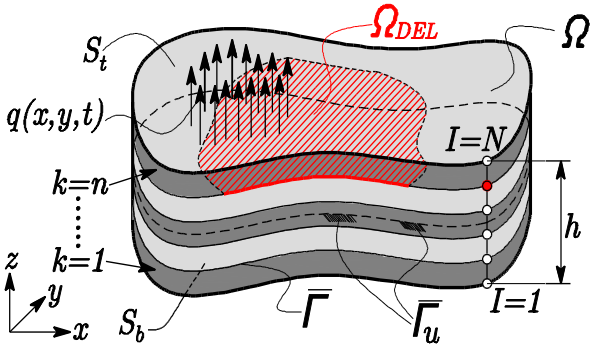

Figure 1.Laminated composite plate with embedded delaminated zone Ω_{DEL}

The Generalized Laminated Plate Theory (GLPT) [15] allows the independent interpolation of in-plane and out-of-plane displacement components and relative displacements of adjacent layers in three orthogonal directions. Piece-wise linear variation of in-plane displacement components and constant transverse displacement through the thickness are imposed (plane stress state). Based on the assumptions of the Generalized Laminated Plate Theory [2-5, 16], the displacement field of an arbitrary point (x,y,z) of the laminate at the arbitrary time instant t is given as:

$$u_1 = u + \sum_{I=1}^{N} u^I \Phi^I + \sum_{I=1}^{ND} U^I H^I$$
$$u_2 = v + \sum_{I=1}^{N} v^I \Phi^I + \sum_{I=1}^{ND} V^I H^I \qquad (1)$$
$$u_3 = w + \sum_{I=1}^{ND} W^I H^I$$

In Eqs. (1), $u(x,y,t)$, $v(x,y,t)$ and $w(x,y,t)$ are the displacement components in the mid-plane of the laminate in directions x, y and z, respectively, $u^I(x,y,t)$ and $v^I(x,y,t)$ are the relative displacements of the I^{th} numerical layer in directions x and y, respectively, and $U^I(x,y,t)$, $V^I(x,y,t)$ and $W^I(x,y,t)$ are the jump discontinuities in the displacement field in the I^{th} delaminated interface in three orthogonal directions. N is the number of interfaces between the layers including S_t and S_b, while ND represents the number of interfaces in which delamination is present. W^I is the Crack Opening Displacement (COD) which is constraint by the non-penetration condition $W^I \geq 0$ in the I^{th} numerical layer. $\Phi^I(z)$ are selected to be linear layerwise continuous functions of the z-coordinate. $H^I(z)$ are Heaviside step functions which describe the delamination kinematics in the I^{th} delaminated layer [2].

The linear strain field associated with the previously shown displacement field can be found in [2, 3, 16]. It serves as the basis for the derivation of $3+2N+3ND$ governing differential equations which define the strong form of the GLPT. The primary variables of the problem are u, v, w, u^I, v^I, U^I, V^I and W^I. To reduce the 3D model to the plate model, the z-coordinate is eliminated by the explicit integration of stress components multiplied with the corresponding functions $\Phi^I(z)$ or $H^I(z)$, introducing the stress resultants which can be found in [16].

Based on the Generalized Laminated Plate Theory, the C^0 layered finite element model consisting of the mid-plane, $I=1,...,N$ numerical layers through the plate thickness (except the middle plane) and finally $I=1,...,ND$ numerical layers in which delamination can occur is derived [16]. Note that only translational displacement components are adopted as generalized displacements.

3. MODELING OF CRACK PROPAGATION

In this work, the displacement field obtained in the conventional finite element calculation is used for the computation of the three modes of the Strain Energy Release Rate along the delamination front using the Virtual Crack Closure Technique, which requires the calculation of the delamination opening behind the front, the nodal forces in the nodes along the front and the virtually closed area in front of the existing delamination. The method is based on the assumptions of the Virtual Crack Closure Technique which are elaborated in [7, 8, 12]. Note that there exists the previously imposed delamination area between two layers of the laminated composite plate, which is conveniently imposed by selecting the nodes in which structural debonding exist (see Figure 2a). The post-processing algorithm presented in this paper should be applied in all nodes of the finite element model after the each calculation step. The procedure is repeated for all delaminated zones in the plate.

3.1 Detection of delamination front

To start, the algorithm detects the ideally bonded nodes in the vicinity of each a priori imposed delaminated node (red dots in Figure 2a). The detected nodes are intact nodes defining the undamaged area of the plate. Nodes dividing the undamaged from the delaminated plate area are the nodes which define the delamination front (blue dots in Figure 2b). The delaminated zone is encapsulated by the polygonal line connecting the nodes along the delamination front (blue line in Figure 2b).

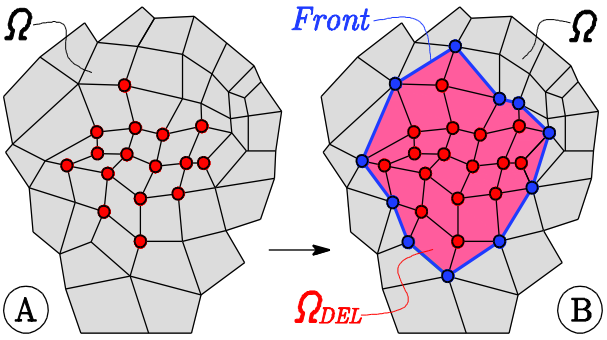

Figure 2. Detection of the delamination front (blue line) according to the debonded nodes (red nodes)

The main advantage of the presented method is its possibility to calculate the orientation of the normal vector $\vec{n}$ defining the direction of the delamination growth. In the majority of the previously proposed models [6, 9, 17, 18], this orientation is assumed a priori. The delamination front in node N is defined by two vectors ($\vec{v}_1$ and $\vec{v}_2$) pointing away from point N to two adjacent points on the delamination front, and dividing the bonded nodes from the debonded ones [12]. After the determination of the vectors $\vec{v}_1$ and $\vec{v}_2$, the vector normal to the delamination front at node N is derived as a unit vector along the symmetry line

defined by $\vec{v}_1$ and $\vec{v}_2$. Having determined the normal vector $\vec{n}$, its corresponding tangent vector $\vec{t}$ is computed based on the vector $\vec{n} = n_x\vec{i} + n_y\vec{j}$ as $\vec{t} = -n_y\vec{i} + n_x\vec{j}$. The vector $\vec{k}$ is the vector perpendicular to the delamination plane. Three unit vectors $(\vec{n},\vec{t},\vec{k})$ form a base of the local coordinate system, in which all G_i components are calculated.

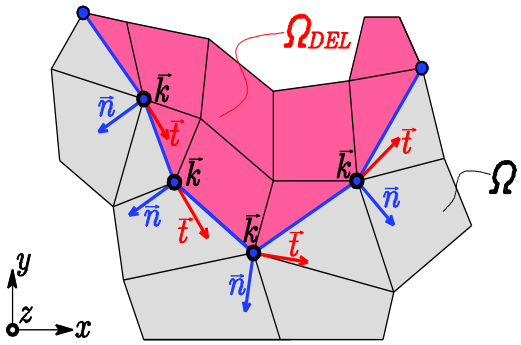

Figure 3. Normal vectors determined at the nodes along the delamination front and the local coordinate system $(\vec{n},\vec{t},\vec{k})$

3.2 Determination of the virtually closed area

To determine G_{I}, G_{II} and G_{III}, the virtually closed area A is calculated using 6 control points for every node N along the delamination front, according to the procedure presented in [12]. The control points P_1-P_3 are known after the calculation of the vectors $\vec{v}_1$ and $\vec{v}_2$, while the control points P_4 and P_5 are derived based on the status of the nodes in the vicinity of current node N. Finally, the point P_6 is derived based on the intersection of directions $\vec{n}$, $\vec{v}_1, \vec{v}_2$ and the locations of points P_4 and P_5. After the six control points P_1-P_6 are determined, the virtually closed area is calculated using the polyarea MATLAB function. Note that an overlap of the virtually closed areas corresponding to the adjacent nodes on the delamination front is a priori prevented.

3.3 Calculation of the Strain Energy Release Rates

After the virtually closed area is determined one needs to compute the forces in the nodes on the crack front, as well as the delamination openings behind the crack front. The forces and the displacements are calculated in the global coordinate system and further transformed in the local coordinate system $(\vec{n},\vec{t},\vec{k})$ located in node N, to reflect the true crack opening mechanism. The delamination openings behind the crack front are calculated in the point P_0, which is anti-symmetric to the point P_6 with respect to the node N. When the point P_0 is defined (see Figure 4), the required jump displacement components are evaluated from the nodal values of the finite element in which the point P_0 is located.

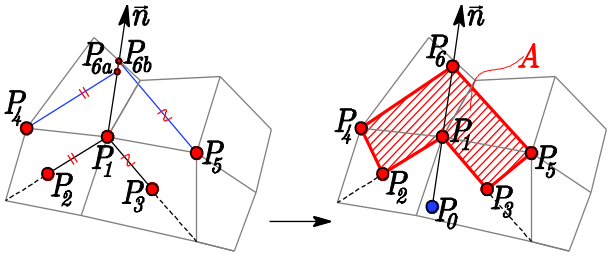

Figure 4. Six control points to determine the virtually closed area A

3.4 Delamination propagation criterion

The three components of the strain energy release rate G_{I}, G_{II} and G_{III} are approximated as the product of the nodal forces at node N (point P_1) and the delamination openings at point P_0, in the region of the virtually closed area A. Once the G_i components are calculated, a mixed-mode fracture criterion for delamination propagation is applied:

$$E_d = \frac{G_I}{G_{Ic}} + \frac{G_{II}}{G_{IIc}} + \frac{G_{III}}{G_{IIIc}} \geq 1 \qquad (2)$$

G_{Ic}, G_{IIc} and G_{IIIc} are the critical values of the strain energy release rate corresponding to Mode I, Mode II and Mode III fracture, respectively. If the above criterion is satisfied, the status of the considered node on the delamination front is changed and the node in which the criterion is satisfied is referred as a *propagating node*. After moving to the next calculation step, the new front is set and the calculation of the G_i components in all nodes along the delamination front is repeated for the same level of loading.

However, the assumption that propagating nodes are only those in which the criterion (2) is satisfied may be quite conservative due to the fact that the assumption of the similarity of the crack before and after the propagation is violated [19]. The proposed method can be easily modified to establish new node-to-node propagation mechanisms (in order to accelerate the solution process and preserve the self-similarity assumption of the VCCT). For details, see Orifici et al. [18].

As previously mentioned, debonding of the boundary nodes is only possible for free (F) plate boundaries, without the possibility to change the previously prescribed essential boundary conditions along Γ_u (e.g. along clamped (C) boundaries). In the proposed method, as soon as

the delamination front reaches the plate boundary the adjacent nodes in the vicinity of the propagating node are also released (see Ref. [18]).

The algorithm is repeated until there are no more propagating nodes in the current step of the analysis. Subsequently, the analysis continues with the next time or loading increment.

4. ALGORITHM FOR PREVENTION OF THE INTERLAMINAR PENETRATION

During the transient response of laminated composite plates with delamination, a small gap may be formed between the adjacent layers in the delaminated zone. During the motion of the plate the embedded delamination may open and close, causing the so-called "breathing phenomenon" [5]. Having in mind that in the presented numerical model a Crack Opening Displacement is stored in a discrete degree of freedom W^I (which generally can reach negative value and cause the penetration of the adjacent layers), the node-to-node frictionless contact algorithm is enforced in every solution step. The details of the implementation of the algorithm are provided in [5]. Note that the contact prevention is activated both in the scenario in which delamination propagation is allowed, as well as in the case of the stationary delamination.

5. NUMERICAL EXAMPLES

5.1 Double-Cantilever-Beam problem

The first validation example is concerned with the well-known Double-Cantilever-Beam (DCB) problem shown in Figure 5. The specimen is assumed to be made of T300/976 graphite/epoxy material with the graphite fibers oriented along the length of the plate (index 1). The following material properties are used in the analysis: E_1=139.3GPa, E_2=E_3=9.72GPa, G_{23}=3.45GPa, G_{12}=G_{13}=5.58GPa, ν=0.29. The critical values of the Strain Energy Release Rates are adopted from Ref. [20] as G_{Ic}=87.6N/m and G_{IIc}=G_{IIIc}=315.2N/m. The cantilever plate is discretized using different mesh densities (50×10 and 75×16) of linear (4-node) and quadratic (9-node) layered finite elements with reduced integration. The boundary conditions are prescribed along the clamped edge by constraining all degrees of freedom along the edge nodes. A delamination zone Ω_{DEL} is prescribed as shown in Figure 5.

In the first part of this example, the plate is loaded by applying Crack Opening Displacements (COD) in 50 steps in equal increments of Δ=0.1mm (see Figure 5). For comparison, the analytical solution of the Double Cantilever Beam test based on the Bernoulli beam theory and Linear Elastic Fracture Mechanics is used [17, 23, 24]:

$$R_{el} = \frac{3}{2}\frac{E_1 \cdot I}{a_0^3}\cdot\Delta, \quad R_{del} = \sqrt{\frac{2}{3}\frac{\left(bG_{Ic}E_1 I\right)^{3/2}}{E_1 I\cdot\Delta}} \qquad (3)$$

In Eq. (3), R_{el} is the linear part of the R-Δ diagram, R_{del} is the nonlinear part of the R-Δ diagram (during the propagation of the delamination), Δ is the prescribed displacement along the free edge of the cantilever, I is the moment of inertia of one part of the cantilever, h is the height of one delaminated part of the cantilever, b=25.4mm is the width of the cantilever, a_0=30mm is the prescribed delamination length and GIc is the critical value of the Strain Energy Release Rate for Mode I. The reaction force is measured in the edge nodes and plotted versus the COD in Figure 6.

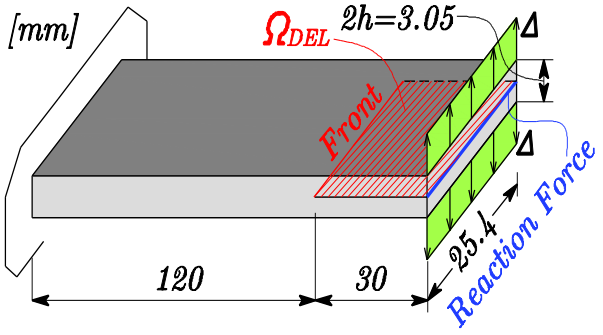

Figure 5. DCB benchmark: Geometry, boundary conditions and prescribed delaminated zone Ω_{DEL}

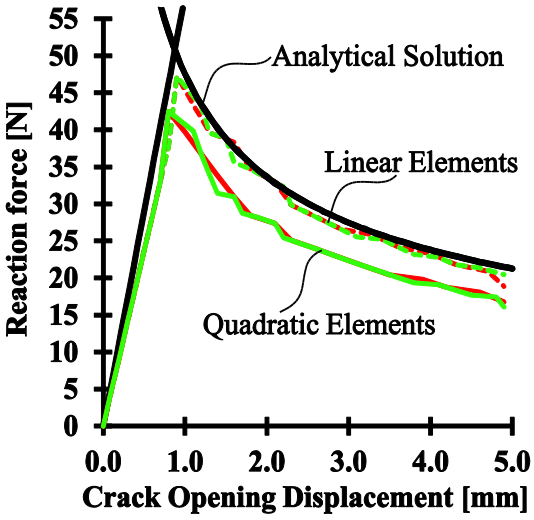

Figure 6. Reaction force versus COD in the Double Cantilever Beam for different element types (red: 50×10 elements, green: 75×16 elements)

Figure 6 shows the comparisons of the numerical and the analytical results of the DCB test for

different mesh densities of the linear and quadratic finite elements. All models generally displayed similar behavior regardless of the mesh size, resulting in i) a linear part of the load-displacement diagram until the initiation of the delamination growth and ii) a nonlinear part where the delamination growth is accompanied by the reduction in the load-carrying behavior.

Mesh refinement generally results in a smoother load-displacement curve because of the shorter distances between two consecutive delamination fronts. Obviously, the elastic branch of the force-displacement curve is slightly softer in the finite element solutions in comparison with the analytical solution based on the Bernoulli beam model (transverse shear deformation is neglected). In addition, the analytical solution accounts only for a single elasticity modulus E_1 ($E_2 = E_3 = E_1$), which also makes the analytical solution slightly stiffer.

Slightly higher values of the reaction force are detected for linear elements – for the quadratic ones the model underestimates the critical forces corresponding to the onset of delamination propagation as compared to the analytical solution due to the same reasons as mentioned above. The study of influence of the mesh density on the G_I distribution along the width of the cantilever plate is presented in [12] and will not be discussed here.

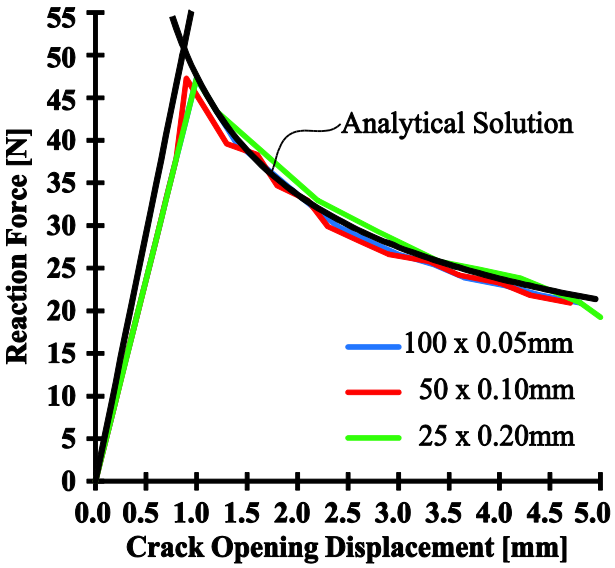

Figure 7. Reaction force versus COD in the Double Cantilever Beam for different sizes of the applied displacement increments

Figure 7 illustrates the reaction force versus the crack opening displacement of the cantilever plate discretized using 50×10 linear elements, for different increments of the applied displacement along the free edge of the cantilever. It is obvious that the reduction of the increment improves the agreement with the analytical solution in the nonlinear portion of the chart, while the influence on the elastic branch is marginal.

The re-analyses of the Double Cantilever Beam benchmark example demonstrated the capability of the proposed plate model to describe both pre- and post-propagation behavior of laminated composite plate in quasi-static conditions.

5.2 Transient analysis of laminated composite plate with a propagating delamination

In this part we investigate the transient response of laminated composite plates with centrally located embedded delaminations of different shape (square or circular). Clamped square composite plates with a side length L=600mm and a thickness h=10mm, composed of four layers (h_k=2.5mm) of carbon-epoxy material in a symmetric stacking sequence (0/90/90/0), are considered. Delaminations are prescribed between layers 3-4 (see Figure 8). The material properties of carbon/epoxy layers are [**11**]: E_1=109.34GPa, E_2= 8.82GPa, G_{23}=3.20GPa, G_{12}=G_{13}=4.32GPa, ν_{12}=ν_{13}=0.342, ν_{23}=0.520, ρ=1500kg/m^3, G_{Ic}=306 N/m, G_{IIc}=632N/m and G_{IIIc}=817N/m.

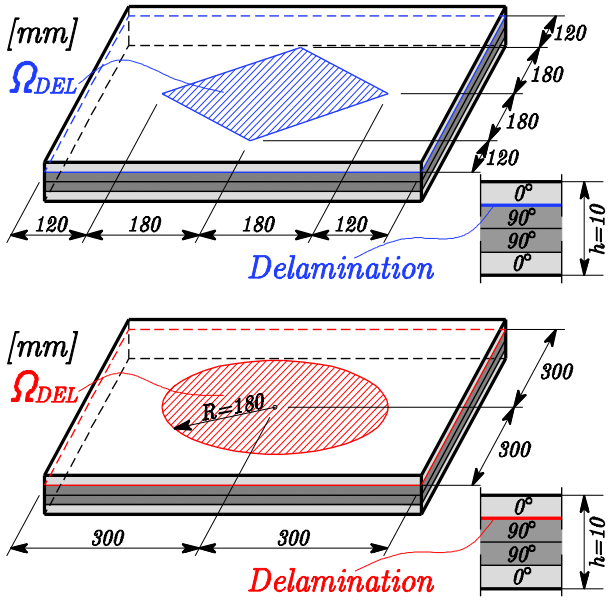

Figure 8. 4-layers (0/90/90/0) cross-ply laminated composite plates with embedded delaminations

A uniformly distributed transverse loading $\boldsymbol{q}$=**75***kPa* is prescribed in the form of a step pulse lasting for $\boldsymbol{T}$=**16***ms*, with a time step $\boldsymbol{\Delta t}$=**0.5***ms* (see [12] for details). The plates are discretized using linear finite elements with the average element size of **20***mm*. The numerical models are generated using the GiD Pre- and Post-processing program (see Figure 9). The element matrices and vectors

are calculated using the reduced Gauss-Legendre quadrature to avoid shear locking (see [3] for details). The extended study of the influence of the mesh density on transient response of delaminated composite plates using the presented model is elaborated in [12]. Note that the mesh refinement does not have a strong influence on the transient response if delamination propagation algorithm is not included [12], resulting only in slightly lower amplitudes and higher frequencies of the delaminated segment.

The transient response is analyzed numerically for the following scenarios: i) composite plate without a delamination (intact plate), ii) the plate with an embedded delaminated zone of different shapes, allowing for delamination growth and, iii) the plate with an embedded delaminated zone of different shapes, suppressing, however, further delamination (the last model is proposed by authors in [5]). The time histories of the transverse deflection of a delaminated layer 4 (see Figure 8) in the center of the plate are plotted in Figure 10 (Δt=0.5*ms*) for different shapes of delamination and different scenarios explained above.

Obviously, due to the presence of an embedded delaminated zone, in the case without delamination propagation as well as in the case, in which delamination growth is enabled, the debonded layer 4 independently oscillates from the intact rest of the plate (layers 1-2-3), resulting in the increase of the amplitudes and the reduction of the frequency in comparison with the intact plate (solid black line in Figure 8).

Considering case ii) (solid blue and red lines in Figure 10), the plate response is considerably changed during the transient motion of the plate in comparison with the numerical model in which the delamination propagation is suppressed (dashed blue and red lines in Figure 10), referred before as case iii). The amplitudes as well as the period of

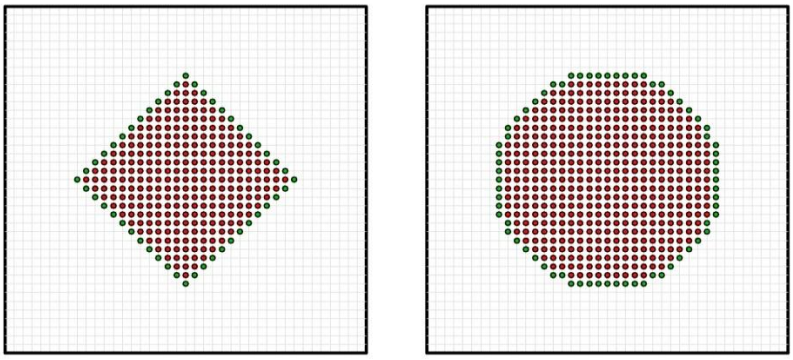

Figure 9: Finite element discretizations for two different delamination shapes (red bullets - prescribed delaminated nodes, green bullets – delamination front)

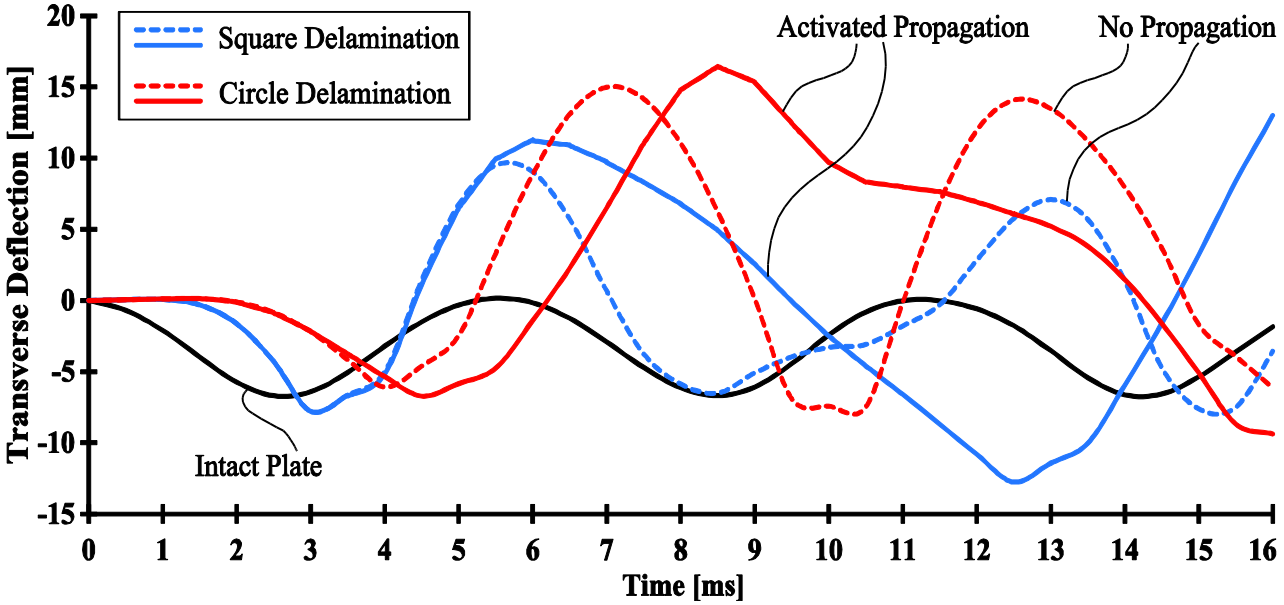

Figure 10: Temporal evolution of the central transverse deflection of the delaminated plate obtained for different delamination shapes and different scenarios regarding the delamination propagation algorithm, for Δt = 0.5ms (solid lines - with delamination growth, dashed lines - without delamination growth)

oscillations are increased in case ii) because of the stiffness degradation caused by the considerable increase of the delaminated area.

The delamination shape severely influences the time point of the initiation of delamination propagation: for the square delamination (blue lines in Figure 10), the delamination propagation begins at approximately t=5.5ms, while for the circled delamination shape (red lines in Figure 10), the propagation starts at app. t=3.0ms. The time point of the start of the delamination growth is detected in Figure 10 as a time point in which considerable difference in time history plot occurs.

Finally, the initial circled delamination is of higher area compared with the square one, which expectedly lead to the softer response and earlier initiation of delamination propagation (difference between blue and red solid lines in Figure 10).

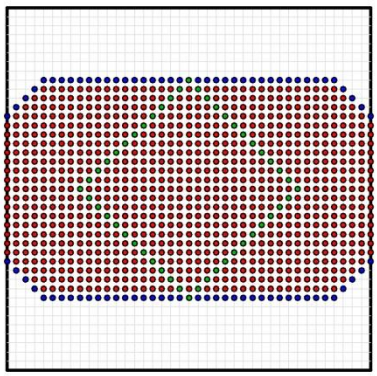

Figure 11. Propagation of the initial square delamination (red bullets - delaminated nodes, green bullets – initial delamination front, blue bullets – final delamination front - t=16ms)

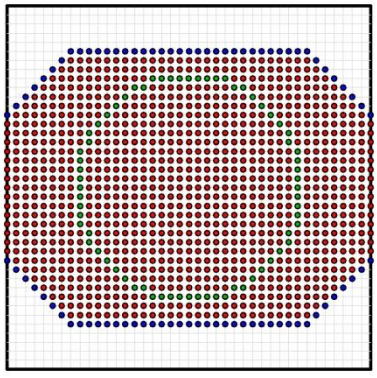

Figure 12. Propagation of the initial circle delamination (red bullets - delaminated nodes, green bullets – initial delamination front, blue bullets – final delamination front - t=16ms)

The final shapes of the delaminated zone at time point t=16ms for both prescribed delaminations are illustrated in Figures 11 and 12. It is obvious that in both cases the prescribed delamination (green bullets in Figures 11 and 12) tends to form an elliptical shape (blue bullets in Figures 11 and 12). The final elliptical shape is formed because of the orthotropic behavior of the composite plate, having the considerably lower properties in x- direction of layer 3 (90^o). The symmetry in the final delamination shape is influenced by the structured mesh of finite elements.

6. CONCLUSIONS

A layered finite element model for static and dynamic computational analysis of delaminated composite plates has been presented. The model has been implemented both for linear and quadratic quadrilateral layered plate elements. Interlaminar penetration between delaminated layers has been prevented by considering contact conditions between the individual layers. A delamination propagation algorithm has been implemented based upon the Virtual Crack Closure Technique to allow for the change of the embedded delaminated zone. The proposed model has been verified and validated by means of analytical solution of the Double Cantilever Beam test. In addition, the model has been applied to the numerical analysis of the transient response of graphite-epoxy composite plates with embedded delaminated zones of different shape. The difference between the presented models with the activated algorithm for delamination propagation, in comparison with the authors' previously derived model in which the delamination growth was not considered, is highlighted. The conclusions have been summarized as follows:

- In the Double Cantilever Beam test, slightly higher values of the reaction force have been obtained, if the model is discretized using the linear elements in comparison with the quadratic interpolation. For the quadratic elements the model underestimates the forces corresponding to the onset of a delamination growth as compared to the presented analytical solution based on the Bernoulli beam theory. Finally, the elastic branch of the force-displacement curve is softer in the presented numerical solution in comparison with the analytical one, because of the incorporation of the transverse shear deformation and the orthotropic behavior of the plate in the numerical solution.
- In the presence of an embedded delaminated zone under dynamic loading, the debonded layer oscillates independently from the intact rest of the plate, resulting in an increase of the

amplitudes and the reduction of the frequency in comparison with the intact plate. This holds for the case without the delamination propagation, as well as for the case in which the delamination growth is enabled.

- Delamination growth severely influences the transient response of the delaminated plate. As soon as a delaminated zone embedded in a composite plate starts to extend when subjected to dynamic loading, the frequency reduces and the amplitude increases considerably as compared to the case, where the growth of the delaminated zone is suppressed.
- The shape of the prescribed delamination influences the transient response of the delaminated segment, as well as the time point of the initiation of the delamination growth. If the prescribed delaminated area is higher, the growth of the delamination starts earlier. This also leads to the softer transient response characterized by the increase of amplitudes as well as of the period.

Future work in this field includes the extension of the presented algorithm to the arbitrary meshes of linear (3-node) and quadratic (6-node) layered finite elements, as well as the implementation of the cohesive law between the initially bonded node-pairs, to simulate the process of debonding more accurately. The thermo-mechanical coupling (the transient response of the delaminated composite plates under the temperature change) should also be considered.

ACKNOWLEDGMENTS

The main part of this research is conducted in a frame of third author's stay at Ruhr University Bochum, Institute for Structural Mechanics, during May-June 2015. The author is grateful to the Institute staff for the valuable remarks and advices which helped to improve the quality of the paper.

REFERENCES

[1] V. V. Bolotin. Mechanics of Delaminations in Laminate Composite Structures. Mechanics of Composite Materials, 37(5), 2001, 367-380.

[2] J. N. Reddy. Mechanics of laminated composite plates: theory and analysis. CRC Press, 1997.

[3] M. Marjanović, Dj. Vuksanović. Layerwise solution of free vibrations and buckling of laminated composite and sandwich plates with embedded delaminations. Composite Structures, 108, 2014, 9-20.

[4] M. Marjanović, Dj. Vuksanović. Free vibrations of laminated composite shells using the rotation-free plate elements based on Reddy's layerwise discontinuous displacement model. Composite Structures, 58, 2016, 80-90.

[5] M. Marjanović, Dj. Vuksanović, G. Meschke. Geometrically nonlinear transient analysis of delaminated composite and sandwich plates using a layerwise displacement model with contact conditions. Composite Structures, 122, 2015, 67-81.

[6] M. Meo, E. Thieulot. Delamination modeling in a double cantilever beam. Composite Structures, 71, 2005, 429-434.

[7] E. F. Rybicki, M. F. Kanninen. A finite element calculation of stress intensity factors by a modified crack closure integral. Engineering Fracture Mechanics, 9, 1977, 931-938.

[8] K. N. Shivakumar, P. W. Tan, J. C. Newman Jr. A virtual crack-closure technique for calculating stress intensity factors for cracked three dimensional bodies. International Journal of Fracture, 36, 1988, 43-50.

[9] F. Shen, K. H. Lee, T. E. Tay. Modeling delamination growth in laminated composites. Composites Science and Technology, 61(9), 2001, 1239-1251.

[10] D. Xie, S. B. Biggers. Strain energy release rate calculation for a moving delamination front of arbitrary shape based on the virtual crack closure technique. Part I: Formulation and validation. Engineering Fracture Mechanics, 73(6), 2006, 771-785.

[11] D. Xie, S. B. Biggers. Strain energy release rate calculation for a moving delamination front of arbitrary shape based on the virtual crack closure technique. Part II: Sensitivity study on modeling details. Engineering Fracture Mechanics, 73(6), 2006, 786-801.

[12] M. Marjanović, G. Meschke, Dj. Vuksanović. A finite element model for propagating delamination in laminated composite plates based on the virtual crack closure method. Composite Structures, 150, 2016, 67-81.

[13] A. J. M. Ferreira. MATLAB Codes for Finite Element Analysis - Solids and Structures. Springer, 2009.

[14] GiD Customization Manual. International Center for Numerical Methods in Engineering, 2016.

[15] E. J. Barbero, J. N. Reddy, J. Teply. An accurate determination of stresses in thick laminates using a generalized plate theory. International Journal for Numerical Methods in Engineering, 29, 1990, 1-14.

[16] E. J. Barbero, J. N. Reddy. Modeling of Delamination in Composite Laminates using a Layer-Wise Plate Theory. International Journal of Solids and Structures, 28(3), 1991, 373-388.

[17] P. Robinson, F. Javidrad, D. Hitchings. Finite element modeling of delamination growth in the DCB and edge delaminated DCB specimens. Composite Structures, 32, 1995, 275-285.

[18] C. Orifici et al. Development of a Finite-Element Analysis Methodology for the Propagation of Delaminations in Composite Structures. Mechanics of Composite Materials, 43, 2007, 9-28.

[19] C. Orifici et al. Development of a degradation model for the collapse analysis of composite aerospace structures. Proceedings of the 3rd European Conference on Computational Mechanics: Solids, Structures and Coupled Problems in Engineering. Lisbon, Portugal, 2006.

[20] H. Hosseini-Toudeshky, S. Hosseini, B. Mohammadi. Delamination buckling growth in laminated composites using layerwise-interface element. Composite Structures, 92(8), 2010, 1846-1856.

[21] H. Hosseini-Toudeshky H, S. Hosseini, B. Mohammadi. Buckling and Delamination Growth Analysis of Composite Laminates Containing Embedded Delaminations. Applied Composite Materials, 17(2), 2009, 95-109.

[22] H. Hosseini-Toudeshky, S. Hosseini, B. Mohammadi. Progressive delamination growth analysis using discontinuous layered element. Composite Structures 92(4), 2010, 883-890.

[23] R. T. Tenchev, B. G. Falzon. A pseudo-transient solution strategy for the analysis of delamination by means of interface elements. Finite Elements in Analysis and Design, 42(8-9), 2006, 698-708.

[24] Y. Mi, M. A. Crisfield, G. A. O. Davies. Progressive Delamination using Interface Elements. Journal of Composite Materials, 32(14), 1998, 1246-1272.